



Estimation of conductivities in a personalized volume conductor model of the human head using MRCDI

Gregersen, Frodi; Eroglu, Hasan Hüseyin; Puonti, Oula; Göksu, Cihan; Siebner, Hartwig R.; Hanson, Lars G. ; Thielscher, Axel

Publication date:
2022

Document Version
Publisher's PDF, also known as Version of record

[Link back to DTU Orbit](#)

Citation (APA):
Gregersen, F., Eroglu, H. H., Puonti, O., Göksu, C., Siebner, H. R., Hanson, L. G., & Thielscher, A. (2022). *Estimation of conductivities in a personalized volume conductor model of the human head using MRCDI*. Abstract from 2022 Joint Workshop on MR phase, magnetic susceptibility and electrical properties mapping, Lucca, Italy.

General rights

Copyright and moral rights for the publications made accessible in the public portal are retained by the authors and/or other copyright owners and it is a condition of accessing publications that users recognise and abide by the legal requirements associated with these rights.

- Users may download and print one copy of any publication from the public portal for the purpose of private study or research.
- You may not further distribute the material or use it for any profit-making activity or commercial gain
- You may freely distribute the URL identifying the publication in the public portal

If you believe that this document breaches copyright please contact us providing details, and we will remove access to the work immediately and investigate your claim.

Estimation of conductivities in a personalized volume conductor model of the human head using MRCDI

Fróði Gregersen^{1,2}, Hasan H. Eroğlu^{1,2}, Oula Puonti¹, Cihan Göksu^{1,3}, Hartwig R. Siebner^{1,4,5}, Lars G. Hanson^{1,2}, Axel Thielscher^{1,2}

¹ Danish Research Centre for Magnetic Resonance, Centre for Functional and Diagnostic Imaging and Research, Copenhagen University Hospital Amager and Hvidovre, Copenhagen, Denmark

² Section for Magnetic Resonance, DTU Health Tech, Technical University of Denmark, Kgs Lyngby, Denmark

³ High-Field Magnetic Resonance Center, Max-Planck-Institute for Biological Cybernetics, Tübingen, Germany

⁴ Department of Neurology, Copenhagen University Hospital Frederiksberg and Bispebjerg, Copenhagen, Denmark

⁵ Department for Clinical Medicine, Faculty of Medical and Health Sciences, University of Copenhagen, Copenhagen, Denmark

Introduction: In MR current density imaging (MRCDI) and MR electrical impedance tomography (MREIT) the current density or conductivity is reconstructed from internal current-induced magnetic flux densities measured with MRI. However, the current density and conductivity reconstruction is challenging due to low SNR, limited volume coverage, and most importantly that only the component of the magnetic flux density parallel to the main field of the MR scanner is measurable (B_z). The “projected current density” method [1] has been used in recent human in-vivo brain MRCDI studies [2–5]. Comparing the results to simulated data we observed that the method only gives very coarse estimates of the “true” current density.

Here we first analyze the accuracy of the projected current density algorithm when used to reconstruct currents in the human head. Secondly, we propose to use an anatomically detailed head model and optimize the conductivities based on the difference between simulated and measured magnetic fields. Parts of the work presented in this abstract have previously been published in a journal article [6].

Methods: The projected current density algorithm attempts to reconstruct the current density from measured magnetic flux density images B_z , and from a simulated current density \mathbf{J}^0 and a magnetic flux density B_z^0 obtained from a model with homogeneous conductivity. The equation derived from Ampère’s law is expressed as

$$\mathbf{J}^{rec} = \mathbf{J}^0 + \frac{1}{\mu_0} \left[\frac{\delta(B_z - B_z^0)}{\delta y}, \frac{-\delta(B_z - B_z^0)}{\delta x}, 0 \right], \quad [1]$$

where the directional derivatives of B_x and B_y are neglected since only B_z is measured in MRCDI. μ_0 is the magnetic permeability of free space. We analyzed the accuracy of the projected current density algorithm with simulated data using

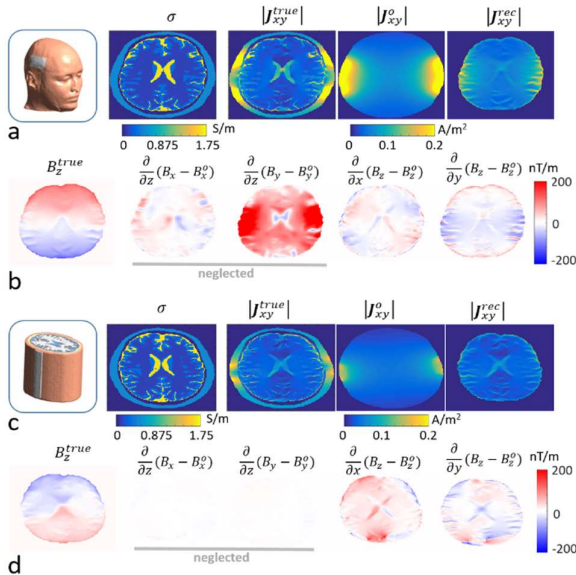


Figure 1: Evaluation of the accuracy of the projection current density algorithm when used on simulated magnetic flux measurements from a human head. a) Simulations based on the *ernie* head model (available as example dataset in SimNIBS) showing the head model, tissue conductivities, true current density, \mathbf{J}^0 used in the algorithm and the reconstructed current density. There is a remarkably clear difference between true and reconstructed current density ($R^2=0.22$). b) The true B_z (simulated measurement), the neglected and used directional derivatives, and the reconstructed current density, respectively. c) same figure as in a, but with a simplified head model with no variation in the z-direction. The similarity between true and reconstructed current density has greatly improved ($R^2=0.63$). d) The B_z and directional derivatives for the simplified head model.

the finite element method (FEM) implemented in SimNIBS 3.1.0 [7]. With a forward simulation using an anatomically detailed head model, the current density was calculated and used as the ground truth to evaluate the current density reconstructed with the projected current density algorithm. A simplified head model with no variation in the z-direction (Fig. 1c) was also used to test the accuracy of the projected current density algorithm for a simpler structure. For the simplified head model, J_z as well as $\delta B_y/\delta z$ and $\delta B_x/\delta z$ from the injected currents, are minimal, rendering all the neglected terms in the projected current density method insignificant.

Instead of reconstructing the current density from B_z , we propose to compare the measured B_z with simulated B_z obtained from a personalized head model with multiple tissue types. The tissue conductivities are then estimated by minimizing the difference between measured and simulated B_z (fig 2). We scanned 5 subjects with two electrode montages (right-left (RL) and anterior-posterior (AP)) using an acquisition-weighted multi-echo GRE acquisition strategy [5]. The five variable tissue types used in the optimization were white matter, gray matter, cortical CSF, skull, and scalp. Ventricular CSF was kept constant to act as an anchor point for the other conductivities since all conductivities can be scaled with a common factor resulting in the same current density and magnetic flux density. To avoid overfitting of the conductivities to individual subjects, we used leave-one-out cross-validation (LOOCV)

where four subjects were used for optimization and the error was evaluated on the remaining subject with the obtained conductivities. Optimization was performed both for RL and AP separately and combined. The error metric was the relative root mean square difference between measurements and simulations.

Results and Discussions: The results from the simulation of the projected current density algorithm using a realistic head model and a simplified head model with no variation in the z-direction are shown in fig. 1a,b and c,d, respectively. The reconstructed current density for the simplified head model ($R^2 = 0.63$) outperforms the reconstruction for a realistic head model ($R^2 = 0.22$). The reason for the poor performance with the realistic head model is clear when visualizing the neglected terms as shown in fig. 1b and d. The neglected terms are much stronger for the realistic head model than for the simplified. J_z is additionally fully ignored by the projected current density algorithm.

In fig. 2 a diagram of the proposed conductivity optimization is shown where the difference between measured and simulated B_z is minimized. An example optimization shows the improved similarity of measured and simulated B_z for the RL montage. Less change is observed for the AP montage. This is also apparent in fig. 3 where the RL errors are larger for all subjects while also displaying a greater reduction of the error after optimization. The improvements for the RL montage for all subjects when using LOOCV indicates a systematic difference between head models and reality that needs to be accounted for in simulations. We have here proposed to use conductivity optimization to increase the robustness of the simulations. However, the obtained conductivities are not necessarily accurate for the given tissue types but do improve the current density simulations for a given electrode montage that gives rise to the simulated B_z . This is further emphasized by the difference in the tissue conductivities for the two electrode positions.

Conclusions: We have here shown that the projection current density algorithm performs poorly for anatomically complex structures such as the human head due to the neglected terms needed for an accurate current density reconstruction. However, for simple structures with little variations in the z-direction, the algorithm provides reasonable results.

We have instead suggested using conductivity optimization of a personalized head model to improve current density simulations for a given electrode montage. Our results indicate a systematic difference between simulation and reality for the RL electrode montage in all five subjects. This can be improved using our proposed method.

References:

- [1] Woo Chul Jeong, Sajib S, Hyung Joong Kim, Oh In Kwon. Focused Current Density Imaging Using Internal Electrode in Magnetic Resonance Electrical Impedance Tomography (MREIT). IEEE Trans Biomed Eng 2014;61:1938–46. <https://doi.org/10.1109/TBME.2014.2306913>.
- [2] Kasinadhuni AK, Indahlastari A, Chauhan M, Schär M, Mareci TH, Sadleir RJ. Imaging of current flow in the human head during transcranial electrical therapy. Brain Stimul 2017;10:764–72. <https://doi.org/10.1016/j.brs.2017.04.125>.
- [3] Chauhan M, Sahu S, Zaman S, Sajib K, Boakye E, Schär M, et al. Current Density Measurements in the Human Brain in-vivo during TES treatment, using Multi- Band methods. ISMRM 28th Annu Meet Exhib 2020.
- [4] Göksu C, Hanson LG, Siebner HR, Ehses P, Scheffler K, Thielscher A. Human in-vivo brain magnetic resonance current density imaging (MRCDI). Neuroimage 2018;171:26–39. <https://doi.org/10.1016/j.neuroimage.2017.12.075>.
- [5] Göksu C, Scheffler K, Gregersen F, Eroğlu HH, Heule R, Siebner HR, et al. Sensitivity and resolution improvement for in vivo magnetic resonance current-density imaging of the human brain. Magn Reson Med 2021:1–16. <https://doi.org/10.1002/mrm.28944>.
- [6] Eroğlu HH, Puonti O, Göksu C, Gregersen F, Siebner HR, Hanson LG, et al. On the Reconstruction of Magnetic Resonance Current Density Images of the Human Brain: Pitfalls and Perspectives. Neuroimage 2021;243. <https://doi.org/10.1016/j.neuroimage.2021.118517>.
- [7] Thielscher A, Antunes A, Saturnino GB. Field modeling for transcranial magnetic stimulation: A useful tool to understand the physiological effects of TMS? Proc Annu Int Conf IEEE Eng Med Biol Soc EMBS 2015;2015-Novem:222–5. <https://doi.org/10.1109/EMBC.2015.7318340>.

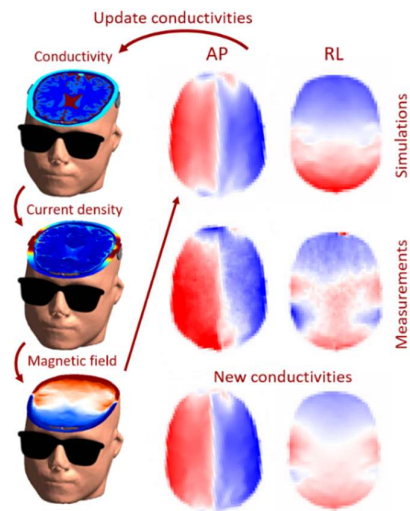


Figure 2: Diagram of the proposed conductivity optimization based on measured and simulated B_z . From a personalized head model with assigned conductivities the current induced magnetic flux density can easily be obtained with a forward simulation. The simulated B_z for a given electrode montage is then compared to measurements and the conductivity of the model is updated to minimize the difference. An example optimization is shown to the right where the B_z maps are obtained from initial conductivities, measurements, and the updated conductivities after optimization, respectively.

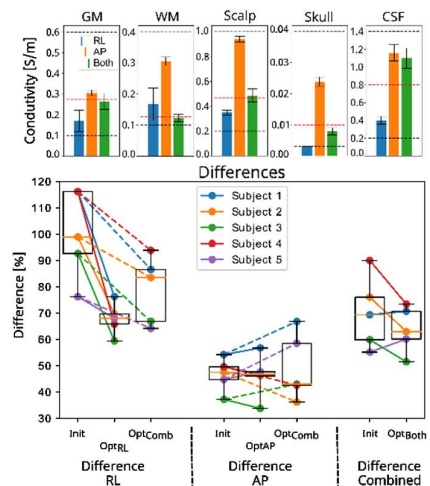


Figure 3: Results from the LOOCV. a) The bar charts show the obtained average conductivities for the 5 optimizations for RL (blue) and AP (orange) electrode montage as well for both montages combined (green). The whiskers are the standard errors and the black and red dashed lines are the conductivity bounds and initial values respectively. b) The differences were calculated for the RL, AP, and both electrode montages, respectively. For each electrode montage, the difference was calculated with initial conductivities (Init), conductivities optimized for one electrode montage (OPT_{RL} or OPT_{AP}), and for both electrode montages combined (OPT_{Comb}).